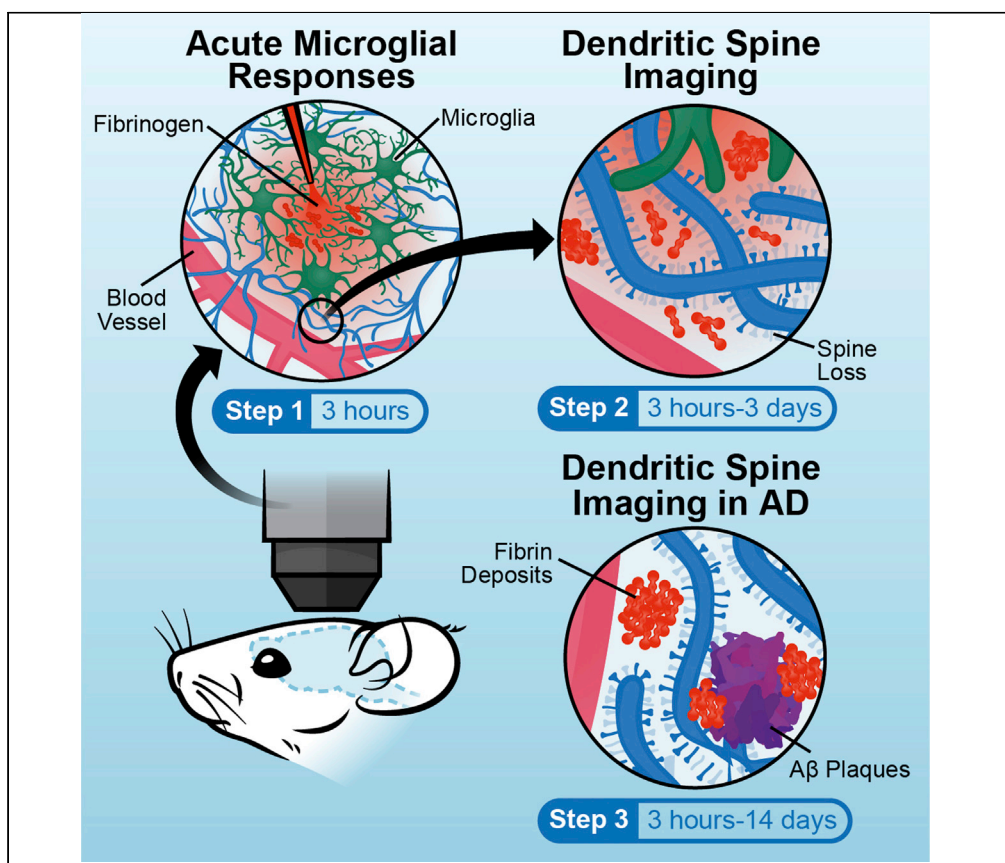


Protocol

In vivo two-photon microscopy protocol for imaging microglial responses and spine elimination at sites of fibrinogen deposition in mouse brain



Deposition of the blood coagulation factor fibrinogen in the central nervous system is a hallmark of neurological diseases with blood-brain barrier disruption. We describe *in vivo* two-photon imaging of microglial responses and neuronal spine elimination to either intracortical microinjection of fibrinogen in healthy mice or to endogenously labeled fibrinogen deposits in Alzheimer disease mice. This protocol allows the longitudinal study of glial and neuronal responses to blood proteins and can be used to test drug efficacy at the neurovascular interface.

Reshmi Tognatta,
Mario Merlini,
Zhaoqi Yan, Renaud
Schuck, Dimitrios
Davalos, Katerina
Akassoglou

reshmi.tognatta@
gladstone.ucsf.edu (R.T.)
kakassoglou@gladstone.
ucsf.edu (K.A.)

Highlights

In vivo two-photon
imaging of acute
microglial responses to
fibrinogen in the
mouse brain

Longitudinal *in vivo*
two-photon imaging of
dendritic spine
elimination to
fibrinogen

In vivo detection of
endogenous
fibrinogen in the brain
by fluorescent dyes

In vivo imaging of
fibrinogen- and
A β -associated spine
elimination in AD mice

Tognatta et al., STAR
Protocols 2, 100638
September 17, 2021 © 2021
The Author(s).
[https://doi.org/10.1016/
j.xpro.2021.100638](https://doi.org/10.1016/j.xpro.2021.100638)

Protocol

In vivo two-photon microscopy protocol for imaging microglial responses and spine elimination at sites of fibrinogen deposition in mouse brain

Reshmi Tognatta,^{1,2,6,7,*} Mario Merlini,^{2,6} Zhaoqi Yan,^{1,2} Renaud Schuck,^{1,2} Dimitrios Davalos,^{3,4} and Katerina Akassoglou^{1,2,5,8,*}

¹Gladstone UCSF Center for Neurovascular Brain Immunology, San Francisco, CA 94158, USA

²Gladstone Institute of Neurological Disease, San Francisco, CA 94158, USA

³Department of Neurosciences, Lerner Research Institute, Cleveland Clinic, Cleveland, OH 44106, USA

⁴Department of Molecular Medicine, Cleveland Clinic Lerner College of Medicine, Case Western Reserve University, Cleveland, OH 44195, USA

⁵Department of Neurology, Weill Institute for Neurosciences, University of California, San Francisco, CA 94158, USA

⁶These authors contributed equally

⁷Technical contact

⁸Lead contact

*Correspondence: reshmi.tognatta@gladstone.ucsf.edu (R.T.), kakassoglou@gladstone.ucsf.edu (K.A.)
<https://doi.org/10.1016/j.xpro.2021.100638>

SUMMARY

Deposition of the blood coagulation factor fibrinogen in the central nervous system is a hallmark of neurological diseases with blood-brain barrier disruption. We describe *in vivo* two-photon imaging of microglial responses and neuronal spine elimination to either intracortical microinjection of fibrinogen in healthy mice or to endogenously labeled fibrinogen deposits in Alzheimer's disease mice. This protocol allows the longitudinal study of glial and neuronal responses to blood proteins and can be used to test drug efficacy at the neurovascular interface. For complete details on the use and execution of this protocol, please refer to Davalos et al. (2012), Ryu et al. (2018), and Merlini et al. (2019).

BEFORE YOU BEGIN

Blood-brain barrier (BBB) disruption and subsequent entry of the blood coagulation factor fibrinogen in the brain is a hallmark of several neurological diseases (Akassoglou and Strickland, 2002). Fibrinogen induces microglial activation (Adams et al., 2007; Davalos et al., 2012) and has been causally linked to neurodegeneration, neuroinflammation and autoimmunity in animal models of Alzheimer's disease (AD), multiple sclerosis, and brain trauma (Merlini et al., 2019; Petersen et al., 2018). Given its pleiotropic functions, fibrinogen represents an emerging target for disease therapeutics (Akassoglou, 2020; Ryu et al., 2018). The protocol below describes the specific steps for *in vivo* two-photon (2P) imaging of microglial responses and neuronal spine elimination to either minimally invasive microinjection of fibrinogen into the cortex or endogenously labeled fibrinogen in cortex of AD mice. However, we have also used this protocol for *in vivo* 2P imaging of microglial responses and spine elimination to plasma from wildtype or fibrinogen-deficient animals, administration of pharmacological inhibitors, *in vivo* 2P imaging of reactive oxygen species (ROS) generation, as well as dynamic microglial-axonal interactions at sites of endogenously labeled fibrinogen in the spinal cord in the experimental autoimmune encephalomyelitis (EAE) model of multiple sclerosis (Davalos et al., 2012; Merlini et al., 2019). This protocol requires a 2P microscope (Ultima IV, Bruker) equipped with a microinjector (Narishige) and a micromanipulator (Narishige).



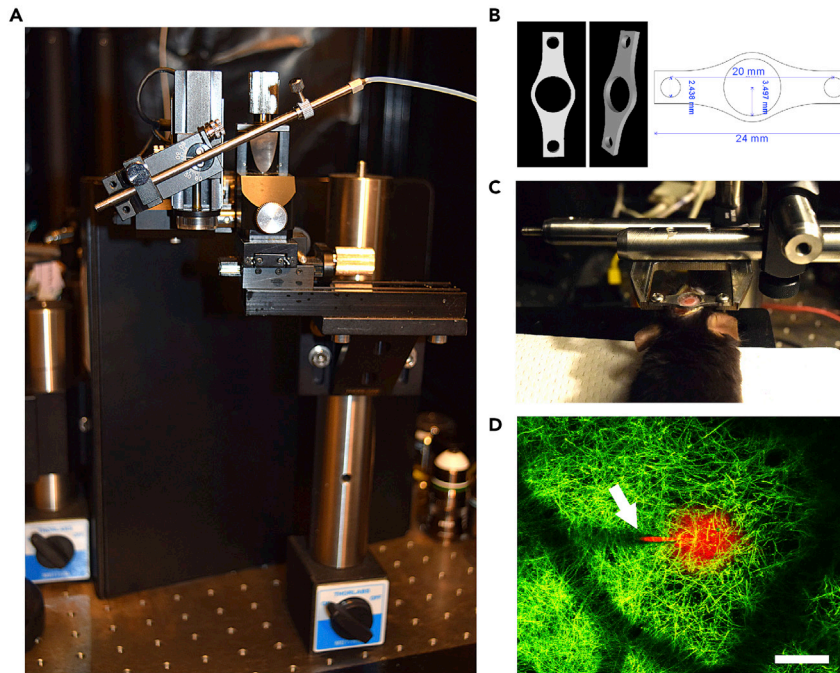


Figure 1. Intracortical microinjection and simultaneous *in vivo* 2P imaging set-up

(A) Photograph of the micromanipulator with microinjection micropipette holder attached to a height-adjustable mounting post. Photograph showing the microinjection setup placed next to the microscope stage.

(B) Schematics and photographs of the custom-made stainless steel cranial headbar with integrated imaging well/chamber. CAD drawings of the custom-made headbar made using the free CAD software from eMachineShop, MahWah, NJ, USA. The two small holes on the side as indicated by the white arrows are for insertion of the screws that attach the headbar/mouse to the holding post.

(C) Photograph of a mouse fixed underneath the microscope by means of the headbar and headbar holding post.

(D) Example of the appearance of a fluorescent “cloud” after successful intracortical microinjection of fibrinogen. Alexa594-labeled fibrinogen (1.5 mg/mL) was delivered 120 μm below dura using the microinjection method described in this protocol during simultaneous acquisition of a z-stack with *in vivo* 2P imaging in a *Thy1-YFP-H* mouse. The microinjected Alexa594-labeled fibrinogen (red cloud-like formation), glass microinjection micropipette (arrow), and dendrites (green-yellow) are visible. Maximum intensity z-projection of a z-stack consisting of 60 z-slices at 1 μm z-step image is shown. Scale bar: 50 μm .

Setup of the microinjector system in the microscope chamber

⌚ Timing: 10 min

1. Attach the needle holder to the micromanipulator following the manufacturer’s instructions provided by info@narishige-usa.com, and use appropriate compressed air tubing to connect a compressed air source to the microinjector and to the needle holder.
2. Mount the micromanipulator bearing the needle holder to a height-adjustable mounting post to allow height adjustment of the needle for intracranial injection (Figure 1A).

Preparation of pulled glass microinjection micropipettes

⌚ Timing: Initial parameter troubleshooting may take several hours. Once parameters are established, ~ 1 min per micropipette

3. Use thin-wall borosilicate glass capillaries with filament; 1.0 mm outer diameter and 0.75 mm inner diameter.
4. Pull microinjection glass micropipettes with a shaft length of 3–5 mm and an outer tip diameter of ~ 1 μm using a micropipette puller at the following settings:

- a. Heat: 560°C (filament temperature ramp +5)
- b. Pull: 45
- c. Velocity: 60
- d. Time: 200

△ **CRITICAL:** Pulling micropipettes with the proper shape, diameter, and tapering angle for efficient penetration of the meninges without breaking of the tip and causing injury to cells or vessels at the pial surface is very important, and may require several trials. It is recommended to invest the time to study how to use a micropipette puller and how to modify parameters to accomplish your desired micropipette shape, and save the successful settings for later use. Also note that settings will need to be adjusted if different glass is used on different occasions. Sharpening of micropipettes can also help with penetration, but is not required.

Preparation of Alexa dye-labeled fibrinogen

⌚ Timing: 50 min

5. In this protocol, we have used Alexa594-conjugated human fibrinogen. Fluorescently-labeled fibrinogen of the appropriate Alexa dye conjugate should be selected for your specific experimental needs, to limit overlap with fluorescence from other cells/structures that will be imaged simultaneously. Prepare a 0.1 M sodium bicarbonate solution by dissolving 0.8175 g sodium bicarbonate in 97.3 mL cell culture-grade water.
6. Filter sterilize the bicarbonate solution under aseptic conditions, e.g., in a tissue culture hood. The filter sterilized bicarbonate solution can be stored at 25°C for 6 months.
7. Add 3.333 mL of the 0.1 M sodium bicarbonate solution prepared above to a 5 mg vial of Alexa dye-conjugated fibrinogen under aseptic conditions in a tissue culture hood. This yields a 1.5 mg/mL Alexa dye-conjugated fibrinogen working solution.
8. Dissolve the Alexa dye-conjugated fibrinogen by rotation-mixing (e.g., use a tissue culture plate shaker) at 200 RPM and 37°C for 30 min, shielded from light (e.g., wrap the vial in aluminum foil). Under these conditions the Alexa dye-conjugated fibrinogen should be completely dissolved within 30 min.
9. Aliquot the Alexa dye-conjugated fibrinogen solution under aseptic conditions in a tissue culture hood.

△ **CRITICAL:** Fibrinogen is a coagulation factor that can clot to an insoluble form and precipitate. Do not place fibrinogen aliquots on ice, and keep the thawed aliquots at 30°C–37°C until ready to inject, as described in steps 42–44.

⏸ **Pause point:** Alexa dye-conjugated fibrinogen solution can be stored at –20°C for 3 months.

Preparation of Methoxy-XO4

⌚ Timing: 20 min

10. Methoxy-XO4 is purchased as a powder (10 mg). Working concentration to be made is 5 mg/mL in 10% DMSO, 45% propylene glycol, 45% PBS, pH 7.5 as follows in steps 11–13.
11. Dissolve Methoxy-XO4 in 200 µL DMSO and invert the bottle several times. Make sure Methoxy-XO4 is fully dissolved.
12. Make the following diluent mixed together PRIOR to adding to the vial with Methoxy-XO4 and DMSO: 900 µL propylene glycol mixed with 900 µL PBS.
13. Slowly add the propylene glycol and PBS mix to the bottle with dissolved Methoxy-XO4. Pipette up and down to mix well.

▮▮ **Pause point:** Methoxy-XO4 can be stored at 4°C, shielded from light for up to 3 months.

Reagent	Final concentration	Amount
Methoxy-XO4	5 mg/mL	10 mg
DMSO	10%	200 µL
Propylene glycol + PBS (pre-mix)	-	900 µL+ 900 µL

KEY RESOURCES TABLE

REAGENT or RESOURCE	SOURCE	IDENTIFIER
Antibodies		
Alexa488-conjugated human fibrinogen, 5 mg vial	Thermo Fisher Scientific	Cat#F13191
Alexa594-conjugated human fibrinogen, 5 mg vial	Thermo Fisher Scientific	Cat#F13193
Alexa647-conjugated human fibrinogen, 5 mg vial	Thermo Fisher Scientific	Cat#F35200
Bacterial and virus strains		
AAV1.hSyn.eGFP.WPRE.bGH	Penn Vector Core	Cat#105539-AAV1
Chemicals, peptides, and recombinant proteins		
Rhodamine B Dextran	Invitrogen	Cat#D1841
Methoxy-XO4	Tocris	Cat#4920; CAS: 863918-78-9
Ketamine, 100 mg/mL	Butler Schein	Cat#010177
Xylazine, 20 mg/mL	Butler Schein	Cat#33197
Buprenorphine	Butler Schein	Cat#031919
Artificial tears/petroleum jelly	Butler Schein	Cat#8897
Betadine	Thermo Fisher Scientific	Cat#19-027132
Metabond Quick Base for dental cement	Parkell	Cat#S398
C Universal TBB Catalyst for dental cement	Parkell	Cat#S371
Clear L-Powder for C&B-METABOND/dental cement	Parkell	Cat#S399
Flow-It ALC	Pentron	N/A
Loctite Ultra Gel Control Super Glue	Office Depot	N/A
Phosphate-buffered saline (PBS)	Thermo Fisher Scientific	Cat#14040-133
Propylene glycol	Thermo Fisher Scientific	Cat#P355-4
Experimental models: Organisms/strains		
Mouse: B6.Cg-Tg(Thy1-YFP)HJrs/J	The Jackson Laboratory	JAX: 003782; RRID: IMSR_JAX:003782
Mouse: B6.129P-Cx3cr1tm1Litt/J	The Jackson Laboratory	AX: 005582; RRID: IMSR_JAX:005582
Mouse: 5XFAD mice (B6SJL-Tg (APPSwFILon, PSEN1* M146L*L286V) 6799 Vas/Mmjax	The Jackson Laboratory	MMRRC#: 34840-JAX; RRID: IMSR_JAX:34840
Others		
Headbar + imaging chamber	eMachineShop, Mahwah, NJ, USA	www.emachineshop.com; N/A
Microinjector system	Narishige, Tokyo, Japan	IM 300
Motorized micromanipulator	Narishige, Tokyo, Japan	MM-80
Micropipette Puller	Sutter Instruments	P-97
Fine-tipped forceps	Roboz	RS-5015
Surgical scissors	Roboz	RS-5606
28-gauge 0.5-mL insulin syringe	Becton Dickinson	Cat#329461
Borosilicate glass capillaries	WPI	Cat# TW100F-6
Ultima IV 2P microscope	Prairie Technologies/Bruker	N/A
Mai Tai eHP DeepSee	Spectra-Physics/Newport	N/A
Insight X3 Ti:sapphire femtosecond laser	Spectra-Physics/Newport	N/A

(Continued on next page)

Continued

REAGENT or RESOURCE	SOURCE	IDENTIFIER
Software and algorithms		
ImageJ, v1. 51	https://imagej.nih.gov/ij/	https://imagej.nih.gov/ij/SCR_003070
MATLAB®, R2018b	MathWorks, Natick, MA, USA	https://www.mathworks.com/products/matlab/ ; SCR_001622
PrairieView, v5.4	Bruker, Middleton, WI, USA	https://www.bruker.com/products/fluorescence-microscopes.html ; N/A

MATERIALS AND EQUIPMENT

Two-photon microscopy

- An Ultima IV 2P microscope (Bruker) equipped with a Mai Tai eHP DeepSee and an Insight X3 Ti:sapphire femtosecond laser (pulse width <120 fs, tuning range 690–1040 nm (Mai Tai) and 680–1300 nm (Insight X3), repetition rate 80 MHz; Spectra-Physics/Newport) is used.
- The lasers are tuned to an excitation wavelength of 840–965 nm depending on the fluorophore(s).
- A Nikon 40× 0.8 NA (working distance: 3.5 mm) or a Nikon 10× 0.4 NA (working distance: 4 mm) water-immersion lens is used for both the microinjection and imaging steps. An Olympus 25× 1.05 NA (working distance: 2 mm) water-immersion lens is used for imaging only.
- Images are acquired at 512 × 512 pixels, 1.5 Hz, and a 1.0 μm z-step.
- The maximum laser power exiting the objective is <40 mW during all imaging experiments.
- An IR-blocking filter and a 520-nm main dichroic are placed in the primary emission beam path before two pairs of detectors. A 573-nm dichroic and a 607/45-nm and 542/27-nm bandpass filter is used to separate Alexa-594/Texas Red/rhodamine and YFP emission, respectively, before the first detector pair; a 458-nm dichroic and a 494/41-nm and 433/24-nm bandpass filter are used to separate GFP and Methoxy-XO4 emission, respectively, before the second detector pair.

△ **CRITICAL:** When performing microinjections, it is essential to use a water-immersion lens with both an adequate working distance and a narrow front lens assembly housing (e.g., the Nikon 10× and 40× water-immersion lenses described here) to allow for sufficient space between the micropipette and the front of the lens. Any contact between the front lens and the micropipette will cause movement of and pressure on the micropipette and likely cause brain damage, and/or possible damage to the front lens.

STEP-BY-STEP METHOD DETAILS

Animal surgery

⌚ Timing: 60–90 min

This section describes steps to expose the brain surface to create a cranial window and fix the head bar to the skull. 2–4 month-old male and female *Cx3cr1^{GFP/+}* and *Thy1-YFP* mice and 7–8 month-old male and female 5XFAD mice and littermate controls are used in this protocol.

1. Use a small-animal heating pad to maintain the mouse body temperature at 35°C–37°C during surgery and imaging.
2. Anesthetize the mouse with an intraperitoneal injection of 100 mg ketamine and 15 mg xylazine (KX) per kg of body weight, diluted in 0.9% NaCl solution prepared under sterile conditions. Adequate depth of anesthesia should be checked regularly during the experiment, e.g., through toe pinching. Supplement with subcutaneous KX injections when needed. In general, subcutaneous KX supplemental doses are 30%–50% of the original dose.

3. Apply artificial tears ointment to the eyes to prevent dehydration of the cornea.
4. Shave the head of the mouse, disinfect the exposed skin with betadine and 70% ethanol, and inject 2% lidocaine (or xylocaine) subcutaneously. Make an incision of approximately 1 cm to expose the skull.
5. Hold the mouse head gently but firmly between thumb and index finger during the following steps.
6. Thoroughly remove subcutaneous connective tissue, clean and dry the exposed skull area.
7. Using a small drill, make a circular moat of about 3–4 mm in diameter over the somatosensory (S1HL/S1FL) cortex until the bone inside the moat flexes under gentle pressure of a dental micro-scalpel blade.
8. Attach a custom-designed steel head bar that includes an imaging chamber (Figure 1B) over the bone island to the skull with cyanoacrylate glue and Metabond dental cement.
9. Apply a drop of pre-warmed (35°C–37°C) artificial cerebrospinal fluid (ACSF, in mM: 125 NaCl, 10 glucose, 10 HEPES, 3.1 CaCl₂, 2.7 KCl, and 1.3 MgCl₂; pH 7.4) to the imaging chamber over the bone island.
10. After about 1 min, gently lift off the bone island with a dental microscalpel blade using the blade as a lever.
11. Gently flush the dura mater with pre-warmed ACSF. Make sure the imaging chamber is covered with ACSF at all times to prevent dehydration of the meninges.
12. For acute cortical microinjection experiments with simultaneous *in vivo* imaging, proceed to “Imaging of acute microglial responses to intracortical fibrinogen microinjection using 2P microscopy” below.
13. For longitudinal imaging experiments that will require revisiting the same cortical area for imaging tissue changes multiple times following intracortical injections, proceed to “Implantation of chronic glass window for longitudinal *in vivo* imaging”.

△ **CRITICAL:** It is recommended that the breathing rate should be regularly checked during the entire course of anesthesia. It is important to frequently stop drilling to prevent overheating the bone and damaging the underlying brain and to use compressed air to clean bone debris, as well as to cool down the bone. Before applying cyanoacrylate glue, the skull should be completely dry to ensure the solid attachment of the headbar. While lifting off the bone island with a dental microscalpel blade, great care should be taken not to touch the brain.

Imaging of acute microglial responses to intracortical fibrinogen microinjection using 2P microscopy

⌚ **Timing:** 1 h

This step describes the *in vivo* imaging of acute microglial responses using Cx3cr1^{GFP/+} reporter mice.

14. Thaw an aliquot of Alexa dye-labeled fibrinogen (see section “Preparation of Alexa dye-labeled fibrinogen”) at 37°C and mix by inverting the tube 2–3 times. It is important to keep the thawed aliquot at 30°C–37°C until ready to inject.
15. Pre-heat a pulled glass microinjection micropipette prepared in step “Preparation of pulled glass microinjection micropipettes” to 37°C and keep at 37°C until ready to inject. Pre-heating can be done by placing the microinjection micropipette on a small animal heating pad or other regulated heating element.
16. If vehicle (e.g., ACSF) solution will be microinjected, mix the solution with a fluorescent dye-labeled dextran to be able to visualize successful injection of the solute into the brain.
17. For imaging the cerebrovasculature, inject a small volume of fluorescently labeled dextran diluted in saline, intravenously (100 µL solution, 3%–5% w/v).

18. Place the mouse on the microscope stage and attach the head bar/imaging chamber to its holder (Figure 1C).
19. Introduce a 25 × or 40 × water-immersion objective lens into the ACSF in the imaging well. The conical tip of the objective should be narrow enough to provide space for the microinjection micropipette.
20. Acquire baseline images of the vasculature in the meninges and the surface of the exposed cortex, as well as of other fluorescent structures that can be used as reference images prior to injection of solutions and/or as maps to relocate the same cortical location in the future.
21. Under epifluorescence light, identify a cortical location that allows insertion of the microinjection micropipette without damage to superficial blood vessels.
22. Raise the objective to create room for insertion of the microinjection micropipette underneath the objective.
23. Back-fill the pre-warmed microinjection glass micropipette with the pre-warmed Alexa dye-labeled fibrinogen solution and insert the micropipette in the injector holder. The angle of the microinjection micropipette should be $\sim 30^{\circ}$ – 35° with tip facing downwards.
24. Introduce the microinjection micropipette into the ACSF filling the imaging chamber, and use epifluorescence to locate the micropipette, center its tip into the field of view of the objective lens, and bring it to focus.
25. Under epifluorescence guidance, gradually lower the injection micropipette with the micromanipulator while simultaneously lowering the objective lens. This has to happen in a gradual and synchronized fashion, to ensure that the micropipette tip and objective lens travel the same distance, so that the micropipette tip remains in the focal plane of the lens. This will allow the user to be always aware of the exact location of the micropipette tip as it is slowly lowered towards the exposed cortical surface.
26. Continue lowering the objective and microinjection micropipette until the dura becomes visible and the micropipette tip is right above it. If available, switch the micromanipulator settings to needle insertion mode, i.e., simultaneous downwards and forwards movement of the micropipette.
27. Using the lowest micromanipulator speed settings, gently insert the micropipette tip through the dura and into the top layer of the underlying cortex.
28. Switch the microscope to 2P laser-scanning mode. Use the 2P laser excitation wavelength, dichroic mirrors, and bandpass filters appropriate for the Alexa dye-labeled fibrinogen or fluorescent dextran-mixed vehicle/ACSF and fluorophores present in the brain.
29. Continue advancing the microinjection micropipette into the cortex until reaching a minimum depth of 70–100 μm below the pial surface.
30. Set the upper and lower limits of a z-stack ensuring that the tip of the micropipette lies in the middle of the stack. Start the z-stack acquisition, and pressure-eject the solution at a pressure of 0.1–0.7 bar and ejection pulse time of 0.5–2 s. The microinjector's ejection pulse time is directly proportional to the volume injected, i.e., increasing the ejection pulse increases the injection volume. Appearance of a fluorescent cloud around the needle tip confirms successful injection (Figure 1D).
31. Set up time-lapse z-stack acquisition parameters using 1 μm z-step, and acquire a full z-stack every 2–3 min for a total of 30 min from injection, for subsequent evaluation of the response of microglial processes to the local injection of fibrinogen.
32. Following the injection, the processes of neighboring microglia invade the area around the injection site and eventually reach the tip of the electrode (Davalos et al., 2005; Davalos et al., 2012) (Figure 2, Methods video S1). To quantify the extent and speed of microglial responses to locally injected fibrinogen:
 - a. Create z-projections of the imaged volumes for each timepoint collected as part of the time-series spanning the microglial response and create the collective timelapse z-stack consisting of all these individual z-projections in sequence.
 - b. To account for signal intensity differences among different experiments, threshold every image in that timelapse z-stack so that all microglial processes have the maximum value 255, and all background is set to 0.

- c. Quantify the number of microglial processes entering from an outer area Y (~70 μm in radius) into an inner area X (~35 μm in radius) surrounding the tip of the electrode as a function of time, by counting the number of white pixels in area X over time ($R_x(t)$) and comparing it with the first picture taken immediately after the insertion of the electrode ($R_x(0)$, measured in the first image of the timelapse). The number of white pixels corresponds to the region covered by processes within the area X, and its increase over time provides a measure of the microglial response. To account for the variability in the number of microglia located in the outer area Y in different experiments, calculate the microglial response relative to the number of processes in the outer area Y immediately after the insertion of the electrode ($R_y(0)$, measured in the first image of the timelapse). The microglial response at any time point ($R(t)$) is therefore given by $R(t) = (R_x(t) - R_x(0)) / R_y(0)$.
- d. Repeat the same procedure for the control (ACSF) injections and plot both responses over time as shown in [Figure 2](#).

Implantation of a chronic glass window for longitudinal *in vivo* imaging

⌚ Timing: 10 min

This section describes steps to implant a chronic glass window on the imaging chamber for longitudinal *in vivo* imaging.

33. Gently flush the craniotomy with ACSF. Place a round glass coverslip (3 mm in diameter, type 0) on top of the dura, making sure it is resting completely on/flush with the dura.
34. Seal the edges of the coverslip with Flow-It™ ALC™ composite and cure the Flow-It™ ALC™ composite under UV light.
35. Follow post-operative care instructions (steps 65–68) and allow 14–21 days for the tissue to recover from the surgery and for the inflammatory response to the cranial window implantation to subside.

Longitudinal *in vivo* 2P imaging of microglial responses and dendritic spine elimination in response to fibrinogen microinjection in healthy mice

⌚ Timing: 1–2 h

This step describes longitudinal *in vivo* 2P imaging of microglial responses, dendrite loss and dendritic spine elimination in layer I-II of the cortex of *Thy1-YFP:Cx3cr1^{GFP/+}* mice ([Methods video S2](#)).

36. To perform intracortical fibrinogen microinjection, follow steps 14–32 of “Imaging of acute microglial responses to intracortical fibrinogen microinjection using 2P microscopy”.
37. Acquire baseline/day 0 images of microglia, dendrites, dendritic spines and the vasculature ([Merlini et al., 2019](#)):
 - a. Set an xyz stack of 100 \times 100 \times 60 μm around the electrode tip, and inject a small volume (5–10 μL) of the respective solution with a pressure injector (Narishige) at a pressure of 0.35–0.6 bar during simultaneous imaging of the neurites, spines, and microglia at 4 \times optical zoom (40 \times objective lens).
 - b. Acquire additional xyz stacks with the 40 \times objective lens at 1 \times and 2 \times optical zoom and with the 10 \times objective lens at 1 \times optical zoom to create overview maps of the vasculature and dendritic structures for relocation of the same imaging site.
 - c. Place and seal a new coverslip over the craniotomy.
38. For re-imaging three days later, anesthetize the mouse with an intraperitoneal injection of 100 mg ketamine and 15 mg xylazine (KX) per kg of body weight, diluted in 0.9% NaCl solution

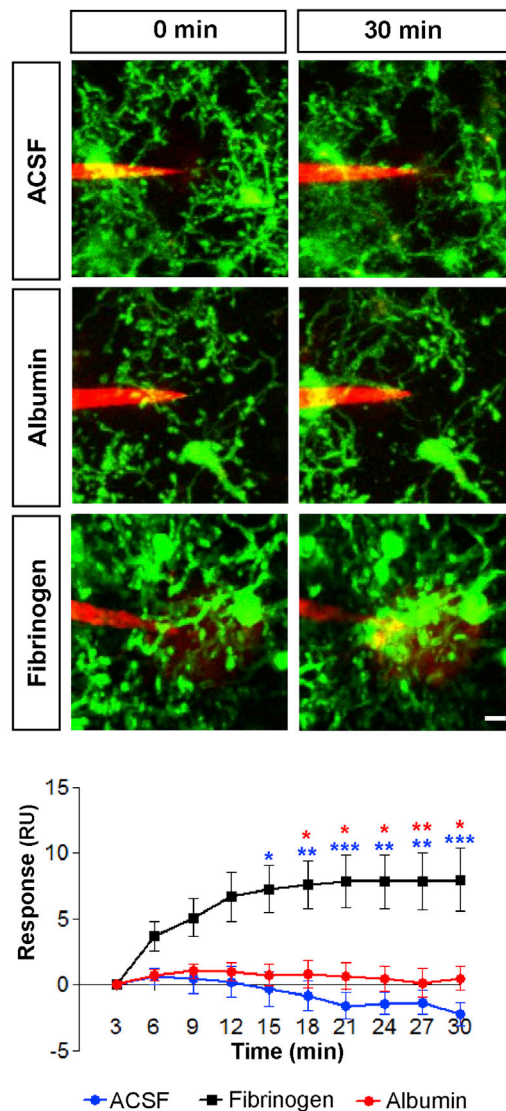


Figure 2. In vivo imaging of fibrinogen-induced microglial responses in the healthy mouse cortex

Local injection of fibrinogen (3–6 mg/mL, red) in the cortex of the *Cx3cr1^{GFP/+}* mice causes microglial process extension (green) toward the tip of the injection electrode; control electrodes containing ACSF, or albumin (5 mg/mL) caused little or no microglial responses. Quantification of microglial responses over 30 min toward the tip of the electrode upon injection of ACSF (n=7 mice), albumin (n=6 mice), or fibrinogen (n=9 mice). Values represent mean \pm SEM. *P<0.05, **P<0.01, ***P<0.001, two-way analysis of variance (ANOVA). Scale bar, 10 μ m. Figure reprinted with permission from [Davalos et al., 2012](#).

prepared under sterile conditions (see section on “Animal surgery” above) and fix the mouse underneath the microscope by attaching the headbar/imaging chamber to the mounting post.

39. To re-image the exact same imaging region(s) of interest (ROIs) follow the ROI re-location method ([Grutzendler et al., 2002](#); [Merlini et al., 2019](#)) (Figure 3):

- a. Use 10 \times and 40 \times vascular overview maps acquired at baseline/day 0 to re-locate the exact ROI.
- b. Identify the location of other fluorescent structures, such as dendrites and dendritic spines) Dendritic spines should be considered the same between two views on the basis of their spatial relationship to adjacent landmarks and their relative position to immediately adjacent spines.

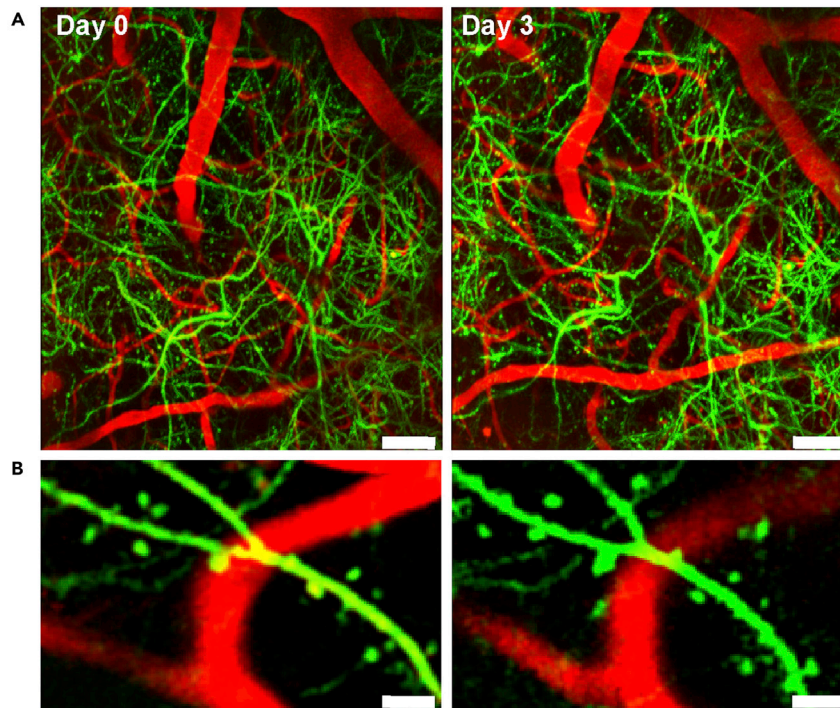


Figure 3. In vivo imaging of vascular and dendritic structures to be used as reference maps for relocating the precise microinjection site for longitudinal imaging sessions

(A) Parenchymal overview images of the brain region in which the microinjection site was located on day 0 / at baseline, and subsequently using characteristic microanatomical shapes of blood vessels (red) and major dendrites (green) the same cortical overview region identified and reimaged three days later.

(B) Magnified images show the experimental data acquired at a depth of about 100 μm directly underneath the dura of the parenchymal overview image FOV. Scale bars in overview images and insets: 50 μm and 10 μm , respectively.

Figure reprinted with permission from [Merlini et al., 2019](#).

40. Repeat post-operative care routine (steps 63–66) and re-image for longitudinal imaging studies.
41. Quantify the long-term effects of the microinjected fibrinogen or vehicle on the dendrites and dendritic spines for each imaging time point, i.e., percentage dendrites remaining and spines lost over baseline/day 0 ([Merlini et al., 2019](#)) (Figures 4A and 4B), as described:
 - a. Process the $100 \times 100 \times 60 \mu\text{m}$ xyz stacks acquired around the glass electrode tip at baseline (day 0/day of micro-injection) and at the same location on day 3 using ImageJ.
 - b. Calculate the number of dendrites at day 3 (injection model) as percentage of that at baseline/day 0.
 - c. To calculate changes or equality in spine numbers at day 3 compared to those at baseline, dendrites should be identified that were present in both the baseline and the day 3 imaging stacks. Calculate the number of spines on these dendrites at day 3 as percentage of that at baseline.
 - d. Quantification should be performed by researchers blinded to the injection agent (fibrinogen or ACSF).

Note: This method can be used for labeling microglia, dendrites and dendritic spines as well as the vasculature using *Thy1-YFP:Cx3cr1^{GFP/+}* mice ([Figure 4C](#)). Fibrinogen microinjection can be performed following steps 14–32 outlined above. In addition, pharmacological inhibitors such as apocynin and knockout mice can be utilized in this experimental design to assess the effects of fibrinogen on microglial responses and spine elimination ([Merlini et al., 2019](#)).

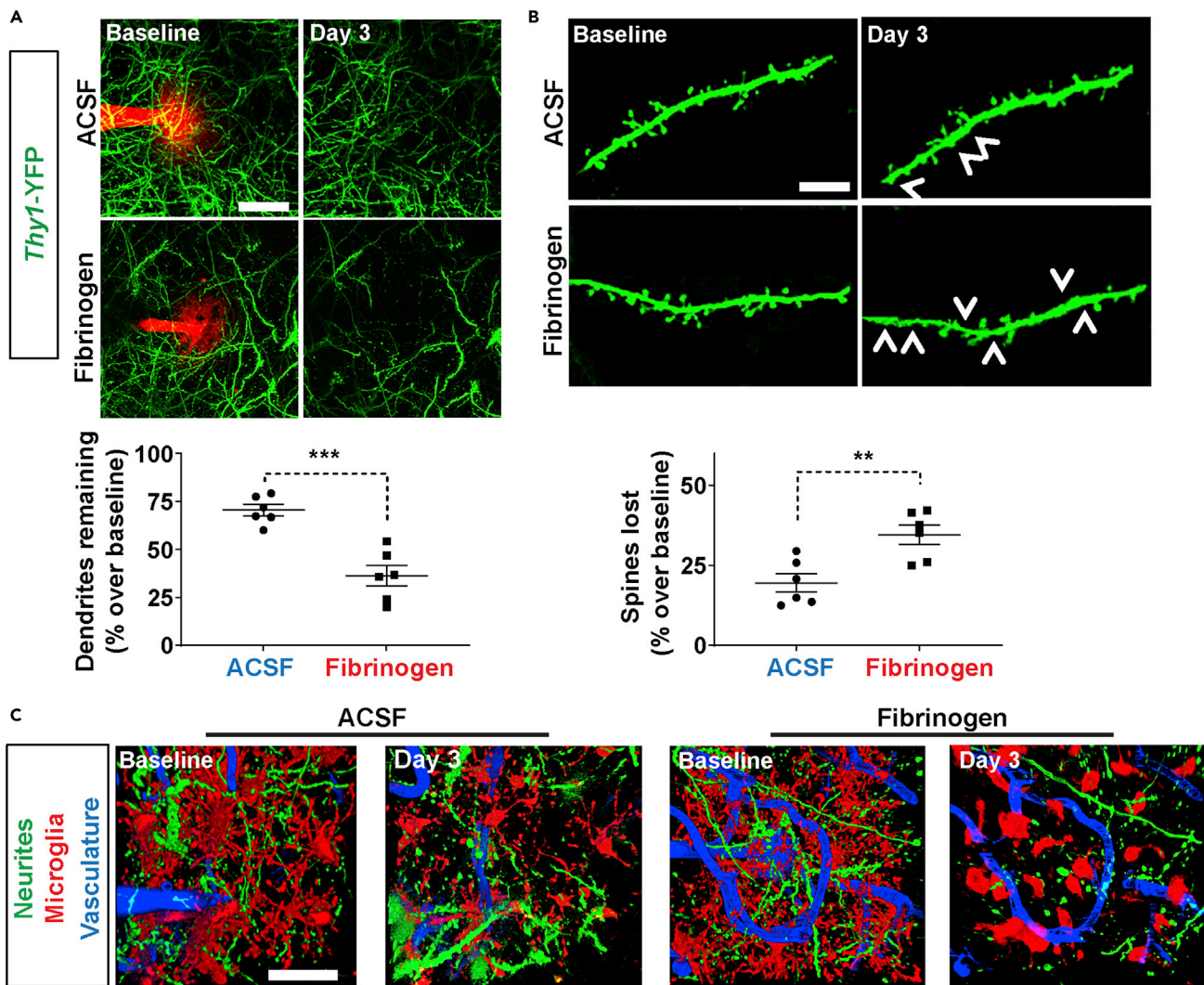


Figure 4. Repetitive, longitudinal *in vivo* 2P imaging of dendrites and spines through a chronic cranial window during and after cortical microinjection of fibrinogen or vehicle control in a *Thy1-YFP-H* mouse

(A) Microinjection of fibrinogen or vehicle (ACSF) (red) on dendrites (green) in the cortex of *Thy1-YFP* mice during injection (Baseline) and three days later (Day 3). Maximum intensity z-projections are shown. Scale bar: 25 μ m.

(B) Longitudinal imaging of dendritic spines (green) and their elimination on day 3 as compared to day 0/baseline are indicated by arrowheads. Maximum intensity z-projections are shown. Scale bar: 10 μ m. Values are mean \pm SEM. ** $p < 0.01$, *** $p < 0.001$ by two-tailed unpaired Student's t-test.

(C) Longitudinal *in vivo* 2P imaging of microglia (GFP, pseudo-colored in red), dendrites (YFP, yellow-green), and blood vessels (Cascade Blue 10kDa dextran, blue) in the cortex of a 12-week-old *Thy1-YFP; Cx3cr1^{GFP/+}* mouse before (Baseline) and after local injection of ACSF vehicle or fibrinogen (Day 3). Representative 3D volume z-projections are shown. Scale bar: 25 μ m. Figure reprinted with permission from Merlini et al., 2019.

***In vivo* fibrinogen labeling: Retro-orbital injections of Alexa dye-conjugated fibrinogen**

© Timing: 5 min

IMPORTANT: Alexa dye-conjugated fibrinogen needs to be administered by retro-orbital (r.o.) injection as outlined below at 48 h (injection 1) and 24 h (injection 2) before the imaging experiment (Figure 5). This protocol has been used for the *in vivo* labeling of fibrinogen in the spinal cord (Davalos et al., 2012) and brain (Merlini et al., 2019; Ryu et al., 2018).

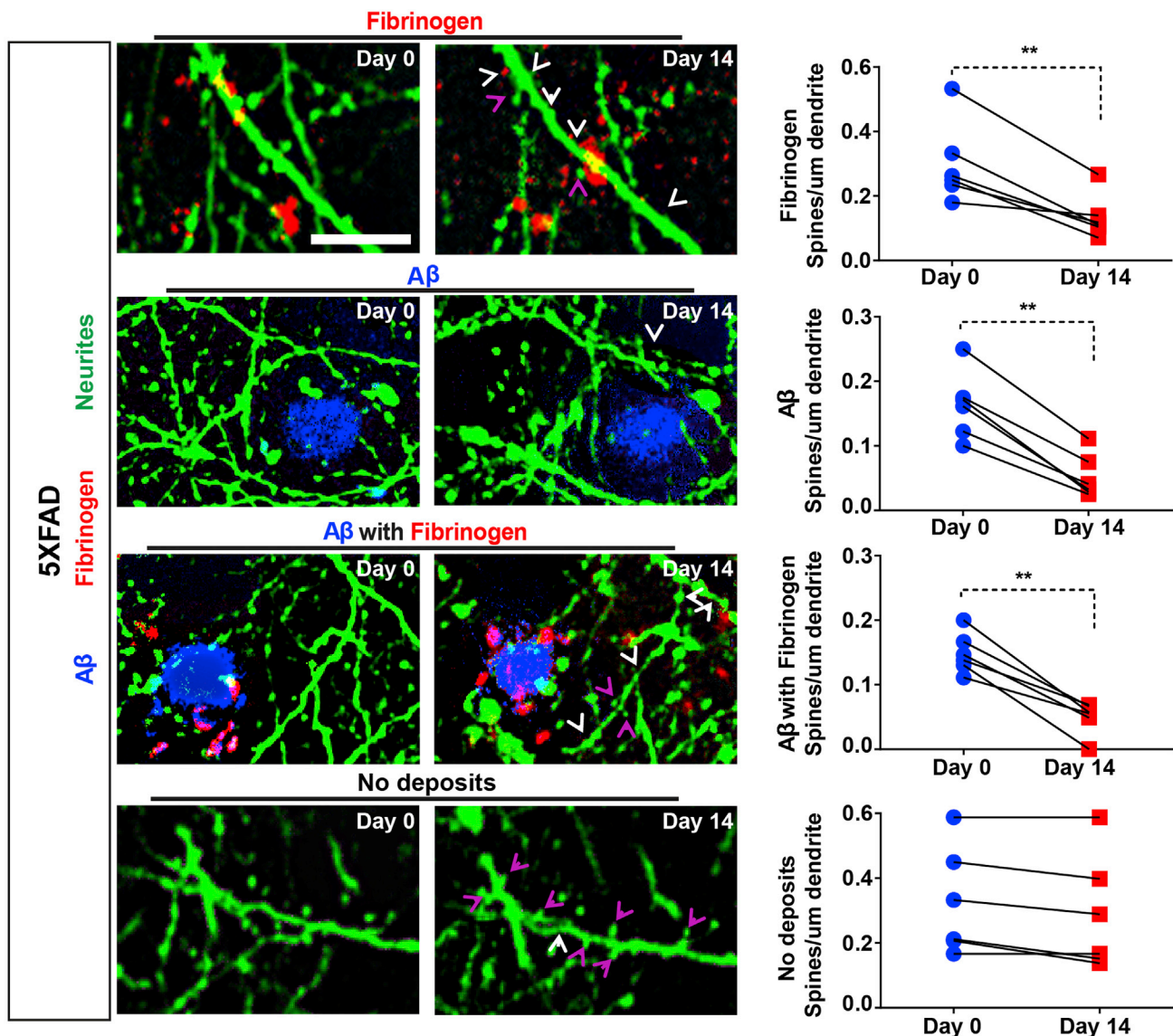


Figure 5. Dendritic spine elimination around fibrinogen deposits in 5XFAD mice

Longitudinal *in vivo* 2P imaging of elimination of spines (AAV-synapsin:GFP, green), fibrinogen (Alexa594-labeled fibrinogen, red), and A β plaques (Methoxy-XO4, blue) in the cortex of 7- to 8-month-old 5XFAD mice following a 14–21-day surgery recovery and virus incubation period. Images were acquired in the same cortical area at both imaging time points. “Day 0” refers to the first day of imaging, i.e., 14–21-day post-surgery. “Fibrinogen,” spines in areas with fibrinogen deposits located $>50 \mu\text{m}$ from A β plaques; “A β ,” spines located within $50 \mu\text{m}$ from A β plaques without fibrinogen deposits; “A β with fibrinogen,” spines located within $50 \mu\text{m}$ from A β plaques with fibrinogen deposits; “no deposits,” spines located $>50 \mu\text{m}$ from either A β plaques or fibrinogen deposits. Arrow heads indicate stable (magenta) and lost (white) spines on day 14 as compared to day 0. Maximum z projections are shown. Scale bar represents $10 \mu\text{m}$. Dendritic spine density was assessed on 30–36 dendrites for each mouse. Values are mean \pm SEM; $n = 6$ mice. $**p < 0.01$ by two-tailed paired Student’s *t* tests. Figure reprinted with permission from Merlino et al., 2019.

42. A volume of $100 \mu\text{L}$ of Alexa dye-conjugated fibrinogen is required for 20–30 g mouse body weight per injection. Thaw the required number of aliquots of Alexa dye-conjugated fibrinogen at 37°C using a heating block. After thawing, invert the solution/aliquot tube 2–3 times.
43. Under light isoflurane anesthesia, i.e., 1.5%–2% isoflurane at an oxygen flow rate of 0.5 L/min, inject $100 \mu\text{L}$ of Alexa dye-conjugated fibrinogen retro-orbitally by inserting a 28-gauge 0.5-mL insulin syringe in the retro-orbital sinus, which is located caudally to each eye.

44. Perform the imaging experiment 24 h after the second injection (see note about injection time points above) using the 2P excitation laser wavelength and emission filter appropriate for the Alexa dye-conjugated fibrinogen used

△ **CRITICAL:** Please see “Preparation of Alexa dye-labeled fibrinogen” steps 5–9 for protocol of fibrinogen preparation. It is recommended to seek training by veterinary staff for proper administration technique in the retro-orbital sinus without damaging the eye. Also, performing the r.o. injection while the mouse is (lightly) anesthetized mice is critical because potential twitching/jerking of the mouse head may cause r.o. vascular damage and, hence, mechanical damage-induced intra-cerebral extravasation of fibrinogen.

Longitudinal *in vivo* 2P imaging of spine elimination around fibrinogen deposits and A β plaques in 5xFAD mice

⌚ Timing: ~2h

This section describes steps for longitudinal *in vivo* 2P imaging of dendrites and dendritic spines around fibrinogen deposits and A β plaques in an AD mouse model.

45. Put the mouse on a temperature-controlled stereotaxic injection frame and fix the head with ear bars.
46. Fill a Hamilton syringe (attached to a beveled 33-G needle) with AAV1.hSyn.eGFP.WPRE.bGH (titer $\geq 7 \times 10^{12}$ vg/mL) to fluorescently label dendritic spines through viral infection.
47. Using a dissection scope, move the syringe to the prefrontal cortical area, lower the syringe until the needle tip touches the skull and record the z coordinate. Perform the same steps for measuring the z coordinate of lambda.
48. Adjust the alignment of the mouse head in the stereotaxic device to yield a < 0.3 mm difference between the prefrontal cortical and lambda z coordinates.
49. Move the syringe to bregma and record the A/P and M/L stereotaxic coordinates.
50. Move the syringe to the somatosensory cortex (in mm from bregma: A/P -0.75, M/L +1.5). Mark location on the skull, then raise the syringe.
51. Drill a hole through the skull at the identified location.
52. Lower the syringe until the tip of the needle touches the dura mater and record the z coordinate. Lower the needle to 1.00 mm below the dura mater.
53. Inject 1 μ L of the virus using an autoinjector set at a speed of 60 nL/min. After the injection, wait 5 min for the virus to diffuse. Slowly raise the syringe and perform “Animal surgery” steps 1–13 and “Implantation of chronic glass window for longitudinal *in vivo* imaging” steps 33–35.
54. Allow a 14-day incubation time for the virus to infect neurons.
55. Perform r.o. administration of fluorescently labeled fibrinogen as described under “*In vivo* fibrinogen labeling: retro-orbital injections of Alexa dye-conjugated fibrinogen” steps 42–44.
56. On day 2 of the r.o. fibrinogen injection, i.e., one day before imaging, administer Methoxy-XO4 (5 mg/kg) by intraperitoneal injection.
57. Use screws to secure head bar with the holder, then fix mouse under the 2P microscope.
58. Use epifluorescence to locate the cranial window.
59. Locate dendritic spines 100 μ m below the dura with and without Alexa 594-labeled fibrinogen deposits and which are located < 50 and > 50 μ m of a Methoxy-XO4-labeled amyloid- β (A β) plaque. Use 2P wavelengths of 840 nm and 920 nm and a 40 \times objective at 4 \times optical zoom.
60. Acquire a stack of 100 \times 100 \times 60 μ m around the region of interest.
61. Acquire additional xyz stacks with the 40 \times objective lens at 1 \times and 2 \times optical zoom and with the 10 \times objective lens at 1 \times optical zoom to create overview maps of the dendritic structures for relocation of the same imaging site.
62. Fourteen days later, locate the same imaging area using the 10 \times and 40 \times vascular overview maps and re-image as described above in steps 38 and 39 (Figure 5).

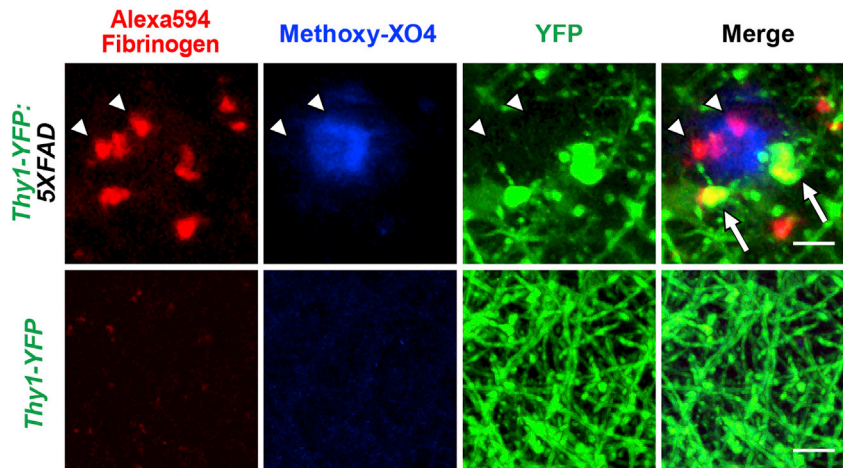


Figure 6. In vivo imaging of fibrinogen leakage and dystrophic neurons in 5XFAD mice

In vivo two-photon imaging of cortex from *Thy1-YFP:5XFAD* mice at 11 months of age shows Alexa594-conjugated fibrinogen (administered intravenously) (red), a methoxy-XO4-positive A β plaque (blue), and dystrophic neurites (green, swollen green structures). Arrowheads indicate fibrinogen (red) surrounding a A β plaque (blue) at areas of neuritic loss. Arrows indicate fibrinogen extravasation at areas of dystrophic neurites (yellow) in proximity to a plaque (blue). Scale bars: 10 μ m. Figure reprinted with permission from (Ryu et al., 2018).

△ CRITICAL: To avoid recording cellular responses due to potential injection-induced brain injury, it is recommended to avoid the needle trace when selecting the ROI for imaging. While drilling the skull at the identified location for viral transfection, it is advised to maintain the minimum widening of the bone surface area necessary for the injection needle and great care should be taken not to touch the dura.

Note: An alternative to labeling of dendritic spines by AAV1.hSyn.eGFP.WPRE.bGH injection (steps 45–54) is the use of *Thy1-YFP:5XFAD* fluorescent reporter mice. Fibrinogen and Methoxy-XO4 labeling can be performed in *Thy1-YFP:5XFAD* mice following steps 55–62 as we previously described (Figure 6) (Ryu et al., 2018).

Post-operative animal care

⌚ Timing: ~1 h

This section describes steps involved in post-operative animal care.

63. Unscrew/detach the head bar from its holder and place the mouse back on the heating pad in the surgery area.
64. Subcutaneously inject 0.5 mL saline as hydration supplement and administer analgesic as recommended by veterinary staff and IACUC, e.g., 0.1 mg/kg buprenorphine.
65. Leave the animal on the heating pad until it has fully recovered from anesthesia. House the mouse individually.
66. Provide analgesia every 6–12 h for 2 days post-operatively or as needed, and as recommended by veterinary staff and IACUC. Daily monitoring of each mouse is required to ensure normal behavior and full recovery from each surgical procedure and imaging session.

△ CRITICAL: Post-operative use of anti-inflammatory drugs such as carprofen or dexamethasone have been shown in prior studies to improve recovery and optical quality of glass windows. However, when performing microglia imaging studies, it is highly recommended

to not use any anti-inflammatory drugs before, during, or after surgery as they may alter microglia morphology and dynamics.

EXPECTED OUTCOMES

For *in vivo* imaging of microglial responses we used *Cx3cr1^{GFP/+}* reporter mice, in which one copy of the CX3CR1 fractalkine receptor gene expressed by myeloid cells is replaced by the gene encoding for the enhanced green fluorescent protein (EGFP), thereby allowing detection of EGFP-expressing cells such as microglia in the brain by fluorescence microscopy (Jung et al., 2000). Acute microglial responses to fibrinogen microinjection through a fine glass micropipette inserted in the cortex of a *Cx3cr1^{GFP/+}* mouse were assessed by simultaneous *in vivo* 2P time-lapse imaging (Figures 1 and 2). The injection “cloud” for Alexa594-labeled fibrinogen is an example of a successful microinjection of Alexa dye-labeled fibrinogen (Figure 1), which is similar to that of ACSF/vehicle mixed with a fluorescent (Texas Red) dextran. By recording the size of the cloud and number of injection pulses used, consistent inter-experiment injection volumes can be achieved (Davalos et al., 2012). Evaluation of microglial responses was performed by measuring the cumulative volume filled by microglial processes over time, using previously published methods (Davalos et al., 2005; Davalos et al., 2012; Merlini et al., 2021). Negligible microglial responses were detected after microinjection of vehicle ACSF mixed with red-fluorescent dextran, indicative of no to minimal tissue damage due to the insertion of the micropipette, using the approach described in this protocol (Davalos et al., 2012).

Repetitive, longitudinal imaging through a chronic cranial window was performed to follow the effects of a few pL of Alexa594-labeled fibrinogen or vehicle control (ACSF) delivered using this protocol on dendritic spine elimination in layer I-II of the cortex of *Thy1-YFP-H* mice. *Thy1-YFP-H* mice express yellow-fluorescent protein (YFP) in several neuronal populations, and predominantly in layer V cortical neurons, also labeling their apical dendrites, and dendritic spines in superficial cortical layers (Feng et al., 2000). Z-series maps of the vasculature and dendritic circuit structures acquired at different levels of magnification on day 0 of imaging (baseline) enable relocation of the same dendrites and dendritic spines at subsequent imaging sessions (Grutzendler et al., 2002; Merlini et al., 2019) (Figure 3). Dendrite loss, dendrites remaining, and dendritic spine elimination, together with microglial responses can be detected and quantified. For the evaluation of dendrite and spine loss in response to fibrinogen, it is important to assess the time-dependent effects of the vehicle control/ACSF to microglia and spines (Figure 4). We performed repetitive *in vivo* 2P imaging of A β plaques, fibrinogen deposits and dendritic spines in the cortex of AD mice over 14 days (Figure 5). Imaging of dendritic spines showed dendritic spine elimination around fibrinogen deposits in AD mice, even in areas distal from A β plaques (Merlini et al., 2019). Finally, we performed *in vivo* imaging of fibrinogen leakage and neuritic dystrophy in AD mice crossed to *Thy1-YFP* mice (Figure 6).

LIMITATIONS

The current protocol describes a highly focal and minimally invasive intracortical microinjection approach, which was specifically developed to be compatible with simultaneous qualitative and quantitative 2P imaging of the neuroinflammatory effects of the blood protein fibrinogen (Iadecola, 2013; Montagne et al., 2017; Petersen et al., 2018; Akassoglou, 2020; Strickland, 2018). This highly localized approach overcomes several limitations of prior methods that introduce blood molecules into the brain, including stereotactic injections, laser-induced cerebrovascular ablations, and dural bathing. Stereotactic injections are prone to cause tissue damage and have relatively low temporal resolution because they cannot be performed simultaneously with *in vivo* imaging. Although laser-induced cerebrovascular ablations are focal and have high temporal resolution, as they can be induced during imaging, they cannot be used to study the effect of a specific blood factor on the brain. Bathing of the dura lacks focal resolution, and penetration of the applied compounds/proteins, especially of large molecular-weight molecules, can be limited to the immediate subdural, superficial cortical tissue. The method described here allows the injection of small volumes (ranging from pL– μ L) of solutions in specific cortical locations, with increased temporal accuracy. In addition,

it allows recording their effects on neighboring cells such as neurons, vasculature, and glial cells in mice expressing fluorescent cell-specific proteins. Furthermore, although it has been optimized for performing injections of fibrinogen, a large, aggregation-prone protein into defined intracortical regions of interest, it can also be employed for the study of acute or sustained localized effects of other proteins or compounds including therapeutic drugs on brain cells or processes. The effects of the microinjected molecules on brain cells of interest can be followed both acutely and longitudinally over several days to weeks, as this method allows repetitive imaging after intracortical delivery of fibrinogen or other large or small molecules including therapeutic drugs through a chronic cranial window. For example, the effects of the NADPH inhibitor apocynin on reactive oxygen species-induced dendritic spine loss were discovered using this method (Merlini et al., 2019).

When injecting aggregation-prone blood proteins like fibrinogen as used in this protocol, the small diameter of the microinjection micropipette tip may become blocked/clogged. As described in the “Troubleshooting” section below, keeping the fibrinogen solution and the microinjection micropipette at 37°C until injection greatly reduces blockage of the needle. Damage to the dura during cranial window surgery can lead to thickening/fibrosis of the dura over time, which degrades the quality of the cranial window and, hence, prevents further imaging experiments. Decreased resolution of the cells or cellular structures, e.g., loss of crisp cell edges and blood vessel walls, and decreased maximum imaging depth compared to that on the first day of imaging are signs of dural fibrosis. Dural fibrosis and/or bone regrowth can also occur if the glass coverslip is not completely flush with/resting on the dura. Vasculitis of the dural and/or leptomeningeal vessels as evidenced by vascular tortuosity, swelling, and/or vessel wall leakage may have inflammatory effects on deeper brain regions, and imaging of mice showing these signs should be discontinued. It is important to note that even though the superficial inflammation occurring as a result of the surgical procedure to implant the window and perform the microinjection should resolve 14–21 days post-surgery, *in vivo* 2P imaging through a cranial window as is required for microinjections is more invasive than imaging through regular thinned-skull or polished and reinforced thinned-skull (PoRTS) windows (Drew et al., 2010; Shih et al., 2012). When experimental conditions require imaging within only a few days after the microinjection and chronic window implantation, it is better to pick a time point within the first 3–4 days, during which the quality of the window can allow the collection of data, and to image at a minimum depth of 100 μm below dura (Merlini et al., 2019). In our experience imaging deeper structures allows more consistent collection of data from brain tissue that can be less affected by the surgical approach. Furthermore, it is critical that controls, sham and vehicle solution injection controls as well as rescue experiments using genetically deficient mice or pharmacological inhibitors are implemented to allow rigorous, quantitative comparisons between treatment and vehicle groups. It is also advisable to complement imaging after direct injection with endogenous labeling of the proteins of interest as described in this protocol. Alternative approaches that allow window implantation with ample time for recovery and microinjections through soft chronic windows or through re-sealable access ports can be used to overcome this limitation (Heo et al., 2016; Roome and Kuhn, 2014).

Injectable anesthetics are commonly administered in rodent surgeries for *in vivo* imaging studies, however, they may alter the function of brain cells, including microglia. Recently, two commonly used anesthetic agents, ketamine/xylazine have been shown to significantly alter microglial process motility as well as their structural complexity *in vivo*. To avoid confounding effects of anesthetics on microglial behavior, *in vivo* imaging of microglial tissue surveillance and process motility can also be performed in awake mice (Liu et al., 2019; Merlini et al., 2021).

While 2P imaging allows the study of acute and long-term inter-cellular interactions and cellular responses pertinent to BBB function, it is beset by the limitation of having a small field of view or sampling range during image acquisition. This small optical window may preclude collection of critical information about the scale and overall pattern of neuroinflammatory and neurodegenerative pathologies throughout different brain regions. The imaging depth that can be accomplished

with most 2P microscopy systems is also limited mostly within the top few layers of cortex due to light scattering and a drop in signal-to-noise ratio with increasing depth, limiting its suitability for imaging deeper structures in the intact mouse brain. However, combining morphological and activity fluorescent reporters compatible with 2P imaging allows for a detailed investigation of neuron-glia interactions and their functional relationships (Merlini et al., 2021).

TROUBLESHOOTING

Problem 1

Blocked needle, no solution is ejected when attempting to inject the fibrinogen solution. This can happen due to fibrinogen conversion to insoluble fibrin within the needle and/or microparticles present in the solution (steps 23–32).

Potential solution

Slowly increase air pressure of microinjector, to a maximum of 20 psi and attempt multiple and/or longer injection pulses. If this does not result in fibrinogen ejection, carefully retract the glass micropipette, fill a new, pre-warmed one with the fibrinogen solution and insert in a new brain location. In some cases, the increased ejection pressure may result in a sudden release of a large volume of the fibrinogen solution, causing brain damage. In these cases, it is not recommended to attempt a new injection or to continue with the experiment in that animal.

Problem 2

The glass micropipette does not fully pierce the dura mater; dura mater is being pushed into the brain parenchyma, apparent as a dark shadow and distorted/blurred field of view (FOV) immediately in front of and around the glass micropipette. Potentially due to blunt glass micropipette tip/incorrectly pulled (steps 26 and 27).

Potential solution

Carefully retract the pulled glass micropipette, fill a new, pre-warmed and of appropriate shape glass micropipette with the fibrinogen or vehicle solution and insert in a new ROI. Consider using tools to sharpen your micropipettes if this happens frequently and you cannot get the micropipette shape to work well, i.e., to accomplish penetration without breaking the tip or severely compressing the meningeal surface.

Problem 3

Acute damage to dendrites apparent as beading/blebbing of dendrites and/or death of microglia apparent as loss of GFP signal within 5–30 min following the injection. Reasons: ejection pressure and/or ejection volume too high, mechanical damage due to lateral movement of glass micropipette, or due to prolonged and excessive tissue compression of the inserted micropipette (steps 31 and 32).

Potential solution

If the size of the induced tissue damage does not cover more than $\frac{1}{4}$ of the entire cranial window, carefully retract the pulled glass micropipette and either reuse or fill a new, pre-warmed glass micropipette with the fibrinogen solution and insert in a new brain region. If the extent of tissue damage detected is extensive, then it is more likely it will affect nearby regions within the cranial window with time, and it is not recommended to attempt a new injection or to continue with the experiment in the same animal.

Problem 4

During longitudinal imaging method/imaging through a chronic cranial window, large leptomeningeal vessels not clearly visible by naked eye, cranial window appears somewhat opaque. This is due to space left between glass coverslip and brain during cranial window surgery, and growth of fibrotic tissue between the dura and glass coverslip (steps 33–35).

Potential solution

In such case it is recommended to terminate the experiment and exclude this animal from the study.

Problem 5

Potential bleeding in the imaging chamber as the bone island is lifted off. Bleeding from blood vessels especially in the imaging chamber can be highly problematic as it obstructs view (step 10).

Potential solution

Carefully flush the dural surface gently with pre-warmed ACSF. It is at times helpful to let the smaller blood vessels bleed out and wait for a clot to form before again attempting to flush away the residual blood. If accidental damage, excessive bleeding or sub-dural bleeding is noticed at this point or if the tissue appears in poor condition after the attempted intervention, it is recommended to exclude this animal from the study.

RESOURCE AVAILABILITY

Lead contact

Further information and requests for resources and reagents should be directed to and will be fulfilled by the lead contact, Dr. Katerina Akassoglou (kakassoglou@gladstone.ucsf.edu).

Materials availability

This study did not generate new unique reagents.

Data and code availability

This study did not generate datasets or code. Any data that support the findings of this study are in the published articles and available from the corresponding author upon reasonable request.

SUPPLEMENTAL INFORMATION

Supplemental information can be found online at <https://doi.org/10.1016/j.xpro.2021.100638>.

ACKNOWLEDGMENTS

We are grateful to Rosa Meza Acevedo, Belinda Cabriga, and Yungui Zhou as well as all prior research associates in the Akassoglou Lab for expert technical assistance with the mouse colony and post-op animal care during the development of these protocols. We thank Giovanni Maki for graphics, Kathryn Claiborn for editorial, and Andrew Mendiola for assistance with figure preparation. This work was supported by a Swiss National Science Foundation Early Postdoc Mobility Fellowship to M.M., grants from the National Multiple Sclerosis Society (RG-1807-32113) and NIH/NINDS R01 NS112526 to D.D., and grants from the Simon Family Trust, the Dagmar Dolby Family Fund, Edward and Pearl Fein, the Conrad N. Hilton Foundation 17348, NIA RF1 AG064926, and NIH/NINDS R35 NS097976 to K.A.

AUTHOR CONTRIBUTIONS

Conceptualization, R.T., M.M., and K.A.; methodology, R.T., M.M., and D.D.; resources, K.A.; imaging and visualization, M.M. and D.D.; manuscript design and organization, R.T. and K.A.; writing, R.T., M.M., Z.Y., R.S., D.D., and K.A.; supervision, funding acquisition, and review and editing, D.D. and K.A.

DECLARATION OF INTERESTS

K.A. is a founder and scientific advisor of Therini Bio. Her interests are managed by the Gladstone Institutes in accordance with its conflict of interest policy.

REFERENCES

- Adams, R.A., Bauer, J., Flick, M.J., Sikorski, S.L., Nuriel, T., Lassmann, H., Degen, J.L., and Akassoglou, K. (2007). The fibrin-derived γ 377-395 peptide inhibits microglia activation and suppresses relapsing paralysis in central nervous system autoimmune disease. *J. Exp. Med.* *204*, 571–582.
- Akassoglou, K. (2020). The immunology of blood: connecting the dots at the neurovascular interface. *Nat. Immunol.* *21*, 710–712.
- Akassoglou, K., and Strickland, S. (2002). Nervous system pathology: The fibrin perspective. *Biol. Chem.* *383*, 37–45.
- Davalos, D., Grutzendler, J., Yang, G., Kim, J.V., Zuo, Y., Jung, S., Littman, D.R., Dustin, M.L., and Gan, W.B. (2005). ATP mediates rapid microglial response to local brain injury in vivo. *Nat. Neurosci.* *8*, 752–758.
- Davalos, D., Ryu, J.K., Merlini, M., Baeten, K.M., Le Moan, N., Petersen, M.A., Deerinck, T.J., Smirnov, D.S., Bedard, C., Hakozi, H., et al. (2012). Fibrinogen-induced perivascular microglial clustering is required for the development of axonal damage in neuroinflammation. *Nat. Commun.* *3*, 1227.
- Drew, P.J., Shih, A.Y., Driscoll, J.D., Knutsen, P.M., Blinder, P., Davalos, D., Akassoglou, K., Tsai, P.S., and Kleinfeld, D. (2010). Chronic optical access through a polished and reinforced thinned skull. *Nat. Methods* *7*, 981–984.
- Feng, G., Mellor, R.H., Bernstein, M., Keller-Peck, C., Nguyen, Q.T., Wallace, M., Nerbonne, J.M., Lichtman, J.W., and Sanes, J.R. (2000). Imaging neuronal subsets in transgenic mice expressing multiple spectral variants of GFP. *Neuron* *28*, 41–51.
- Grutzendler, J., Kasthuri, N., and Gan, W.B. (2002). Long-term dendritic spine stability in the adult cortex. *Nature* *420*, 812–816.
- Heo, C., Park, H., Kim, Y.T., Baeg, E., Kim, Y.H., Kim, S.G., and Suh, M. (2016). A soft, transparent, freely accessible cranial window for chronic imaging and electrophysiology. *Sci. Rep.* *6*, 27818.
- Iadecola, C. (2013). The pathobiology of vascular dementia. *Neuron* *80*, 844–866.
- Jung, S., Aliberti, J., Graemmel, P., Sunshine, M.J., Kreutzberg, G.W., Sher, A., and Littman, D.R. (2000). Analysis of fractalkine receptor CX3CR1 function by targeted deletion and green fluorescent protein reporter gene insertion. *Mol. Cell. Biol.* *20*, 4106–4114.
- Liu, Y.U., Ying, Y., Li, Y., Eyo, U.B., Chen, T., Zheng, J., Umpierre, A.D., Zhu, J., Bosco, D.B., Dong, H., et al. (2019). Neuronal network activity controls microglial process surveillance in awake mice via norepinephrine signaling. *Nat. Neurosci.* *22*, 1771–1781.
- Merlini, M., Rafalski, V.A., Ma, K., Kim, K.Y., Bushong, E.A., Rios Coronado, P.E., Yan, Z., Mendiola, A.S., Sozmen, E.G., Ryu, J.K., et al. (2021). Microglial Gi-dependent dynamics regulate brain network hyperexcitability. *Nat. Neurosci.* *24*, 19–23.
- Merlini, M., Rafalski, V.A., Rios Coronado, P.E., Gill, T.M., Ellisman, M., Muthukumar, G., Subramanian, K.S., Ryu, J.K., Syme, C.A., Davalos, D., et al. (2019). Fibrinogen induces microglia-mediated spine elimination and cognitive impairment in an Alzheimer's disease model. *Neuron* *101*, 1099–1108 e1096.
- Montagne, A., Zhao, Z., and Zlokovic, B.V. (2017). Alzheimer's disease: A matter of blood-brain barrier dysfunction? *J. Exp. Med.* *214*, 3151–3169.
- Petersen, M.A., Ryu, J.K., and Akassoglou, K. (2018). Fibrinogen in neurological diseases: mechanisms, imaging and therapeutics. *Nat. Rev. Neurosci.* *19*, 283–301.
- Roome, C.J., and Kuhn, B. (2014). Chronic cranial window with access port for repeated cellular manipulations, drug application, and electrophysiology. *Front. Cell Neurosci.* *8*, 379.
- Ryu, J.K., Rafalski, V.A., Meyer-Franke, A., Adams, R.A., Poda, S.B., Rios Coronado, P.E., Pedersen, L.O., Menon, V., Baeten, K.M., Sikorski, S.L., et al. (2018). Fibrin-targeting immunotherapy protects against neuroinflammation and neurodegeneration. *Nat. Immunol.* *19*, 1212–1223.
- Shih, A.Y., Mateo, C., Drew, P.J., Tsai, P.S., and Kleinfeld, D. (2012). A polished and reinforced thinned-skull window for long-term imaging of the mouse brain. *J. Vis. Exp.* *61*, 3742.
- Strickland, S. (2018). Blood will out: vascular contributions to Alzheimer's disease. *J. Clin. Invest.* *128*, 556–563.